Reprinted without change of pagination from the
Proceedings of the Royal Society, A, volume 270, *pp.* 366–385, 1964

The air velocity in blast waves from t.n.t. explosions

By J. M. Dewey

The air velocity in blast waves from t.n.t. explosions

By J. M. Dewey

Suffield Experimental Station, Alberta, Canada

(*Communicated by A. G. Gaydon, F.R.S.—Received 29 October* 1963)

[Plate 9]

The air velocity has been measured in blast waves produced by the detonation of trinitrotoluene (t.n.t.) charges varying in mass from 30 to 200000 lb. The technique consists essentially of using a high-speed camera to record the displacement of smoke trails formed close to the charge just before detonation. The initial decay of velocity behind the shock agrees well with theoretical predictions, such as those of Brode (1959), but at later times there is an extended outward flow, which, it is postulated, is caused by the 'after-burning' of the detonation products in the presence of atmospheric oxygen. It has been shown that this phenomenon does not occur in the case of the detonation of an explosive with a high oxygen balance, or for a nuclear detonation. The velocity decay within a t.n.t. blast wave may be described by the equation

$$V = V_s(1-\beta t)\exp(-\alpha t)+a\ln(1+\beta t)$$

fitted to the data by an iterative least squares procedure. It has been demonstrated that particle trajectories, determined by the smoke tracer technique, may be used to calculate the variations of density, pressure and temperature within the wave, without reference to other measurements.

1. Introduction

Sir Geoffrey Taylor (1950) calculated the basic characteristics of an intense point source explosion of negligible mass, and was able to describe the resulting blast wave to the time at which the peak hydrostatic pressure had fallen to about 10 atm. At lower pressures his analysis ceased to be accurate because the similarity assumptions that he had used to describe the blast wave were valid only when the peak pressure was large compared to the ambient atmospheric pressure. Von Neumann & Bethe (1958) made similar calculations and, in addition, gave a mainly qualitative description of the point source blast wave in intermediate and low pressure regions by assuming in the first case that $\gamma-1$ was small, and for the low-pressure region that an approximate acoustical theory could be applied. This theoretical work has been further extended by Sakurai (1953, 1954) and Oshima (1960). The advent of high-speed digital computers made it possible to carry out complete numerical solutions for the spherically symmetrical explosion. Results of such analyses were reported by Broyles (1960) and Brode (1955) for a point source, and Brode has made similar calculations for the explosion of high-pressure spheres (Brode 1956) and spherical trinitrotoluene (t.n.t.) charges (Brode 1959). These calculations are particularly valuable because they give not only the shock front conditions but also the predicted variation of pressure, density, temperature and particle velocity throughout the region from the charge centre to the shock front.

In 1956, a programme was started at Suffield Experimental Station, Canada, to study the physics of blast waves, using mainly charges of t.n.t. ranging in size from 8 to 10^6 lb. Until that time the blast parameter most commonly measured

FIGURE 1. Smoke trails displaced by the blast wave from a 200000 lb. t.n.t. surface burst charge; 110 ms after detonation.

(*Facing p.* 368)

had been the hydrostatic overpressure. The peak value could be determined from the shock velocity, and the decay with time by means of piezo-electric transducers. Many of the effects associated with blast waves arise from the dynamic pressure of the air flow after the passage of the shock front, and for this reason studies were started to determine the air density and velocity in this region. A gauge which has been developed to determine the density has been described by Dewey & Anson (1963), and the techniques and results of the velocity measurements are the subject of this paper.

2. Experimental techniques

Initial studies of blast waves at Suffield Experimental Station were concentrated on the region in which the peak side-on overpressure varies from about 7·5 to 0·5 atm. This is the region of most interest to those concerned with the response of structures to blast waves. At peak overpressures of 7·5 and 0·5 atm the Rankine-Hugoniot equation yields peak particle velocities of approximately Mach 2 and 0·3 respectively, relative to the speed of sound ahead of the shock, and these values might be expected to decay to zero in times of about 10 to 200 ms for the range of explosive yields considered. The violent accelerations involved have precluded the use of any normal type of anemometer, although Ström (1962) has described a corona discharge absolute anemometer which might be used for this purpose. The technique developed at Suffield uses high-speed cameras to record the movement of visible low inertia tracers. In conjunction with this work, Muirhead, Lecuyer & McCallum (1959) and Muirhead & Lecuyer (1959), measured the movement of various types of smoke streams in shock tube flows, and within the limits of experimental error showed that they acted as perfect tracers of the air flows. This technique was later extended to study the air flows associated with the interaction of shock waves with a variety of small-scale structures (Muirhead & McCallum 1959).

The method, as developed for use in the field with large yield explosions, consisted of forming smoke trails in a vertical plane containing the charge centre and parallel to the object plane of a high-speed ciné camera. The displacement with time of the trails was measured from the resulting films; the air velocity was then calculated, and subsequently transformed from Lagrangian to Eulerian co-ordinates to give the velocity-time variation at specific distances from the explosion. A typical set of smoke trails is shown in figure 1, plate 9, which is a photograph taken 110 ms after the detonation of a 200000 lb. surface burst hemispherical charge of t.n.t.

The trails were formed by a chloro-sulphonic acid mixture released from spinning mortar shells consisting essentially of steel tubes sealed at both ends, as shown diagrammatically in figure 2. Two holes in the walls of the tube, close to the leading end are sealed internally by a metal plug silver soldered into position. A 7 g hammer is held by a brass shear wire in a hole drilled into the threaded plug which seals the shell. At the lower end there is an impulse turbine. The shell is fired by means of a 25 g gunpowder charge contained in a cartridge, and the resulting explosion gives the shell an initial velocity of about 700 ft/s and an angular velocity of about 400 rev/s. The hammer at the upper end is released by the impulsive motion of the shell, and strips off the metal plugs. The deceleration by air resistance, and the

centrifugal forces of the spinning shell ejects the 30 ml. of acid mixture through the unplugged holes. The acid rapidly absorbs atmospheric water vapour to form an acid droplet trail about 2 ft. wide. The mortars are fired a few tenths of a second before the charge is detonated to produce trails of the desired height immediately before the arrival of the shock front.

In order to determine accurately distances in the plane of the smoke trails, marker boards were placed at intervals along the mortar line. These were made from steel plates supported by girders set in concrete, so that they were not displaced by the blast wave. The surface of each plate was painted with a black and white pattern and the distance and elevation of the pattern centre was surveyed relative to the charge centre.

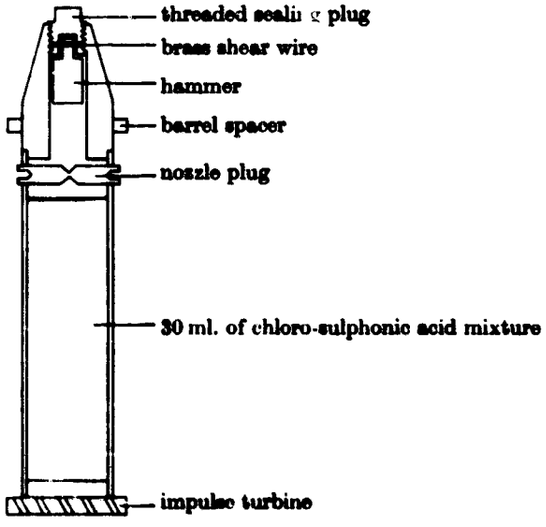

FIGURE 2. Diagram of smoke mortar shell.

In the majority of experiments two 16 mm cameras were used to record the smoke movement; a Fastax WF3T operating at between 2000 and 4000 frames/s, and a high-speed Kodak operating in the range from 1000 to 3000 frames/s. Neon bulbs within the cameras marked the edges of the films, using a pickup from the detonation pulse to obtain a zero signal, and the output from a crystal oscillator to give timing marks at 1 or 2·5 ms intervals.

All the experiments described here were carried out in bright sunny conditions, and it was found that the contrast of the smoke trails against a clear or hazy sky was so slight that the trails could be studied only during a short period in which they were illuminated by the fireball. In order to improve the contrast, the trails were photographed against a black smoke background formed by burning petrol, gelled by adding 2% Octoic acid and 4% Octal powder.

3. Analytical procedures

The individual frames of the films were projected at a magnification of approximately 20. The charge centre was not normally in the field of view, but its position in the projection plane could be determined from those of the marker boards. A

grid of radial lines was drawn on the projection plane through this point. Each frame was projected onto the grid and alined correctly by positioning the images of the markers. A typical grid and frame is shown as figure 3.

It was assumed that the air movement was radial so that the intersection of a smoke trail and a grid line defined a smoke element, the motion of which could be followed from frame to frame. The assumption of radial movement has been confirmed in several experiments in which intersecting patterns of smoke trails in the same plane were used, so that the movement of each intersection could be observed.

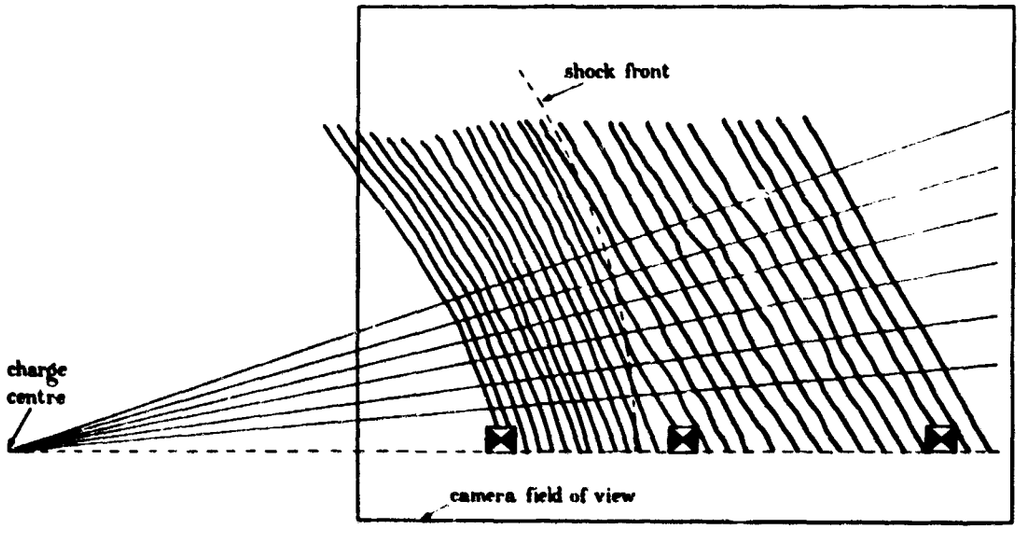

FIGURE 3. Smoke trail pattern projected on to radial grid. The intersection of a trail and a grid line defines a smoke element the displacement of which from the charge centre may be measured. The camera field of view is that used for a 10000 lb. t.n.t. experiment with trails formed at a nominal elevation of 60°. The centre marker board was 185 ft. from the charge centre.

In all cases of ground burst hemispherical charges the movement was found to be radial over the region of displacement of a single intersection. A complete pattern of intersecting trails was not normally used in these experiments since it entailed a much wider grid spacing and a corresponding reduction in the quantity of data obtained. The technique has been used, however, in cases where the flow was not expected to be radial, such as for venting underground explosions.

The horizontal distance of each element from the charge centre was measured with the aid of a film reader consisting essentially of a potentiometer giving a digital output on punched paper tape. References labelling the trail, grid line and the time after charge detonation were also coded. The displacement-time measurements of each element were then sorted from the total data by means of a digital computer. At this stage the horizontal component of an element displacement was corrected for the effects of wind, and resolved to give its radial displacement from the charge centre. In each experiment the wind speed and direction were monitored continuously at a limited number of positions and heights. Owing to spatial variations, however, it has been found far more reliable to determine the specific wind

component in the plane of the trails by measuring their drift before the arrival of the shock. No experiments were carried out with winds of greater than about 10 miles/h.

A fourth-degree polynomial was then fitted to the displacement-time data for each smoke element. The fit was made only up to the arrival of the secondary shock, at which point there is a discontinuity of the first derivative. Figure 4 shows a typical set of data and the resulting fitted curve.

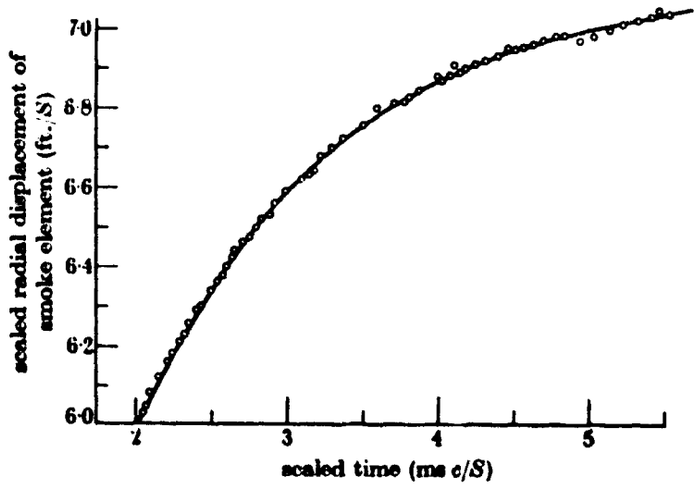

FIGURE 4. Variation of particle displacement with time. Points are the observed values. Line is the fit to a fourth-degree polynomial.

The standard error of such fits varied from 0·08 ft. for 60 lb. charges to 0·5 ft. for a 100-ton charge, and these figures are probably the best indication of the accuracy with which a trail centre could be defined. From this point of the analysis the parameters were scaled as follows. Radial distances, r, were reduced to r/S and times, t, to ct/S, where $S = \sqrt[3]{(WP_0/P)}$; c was the ambient velocity of sound, W the charge mass in pounds, P the atmospheric pressure, and P_0 a standard pressure, taken for the altitude of Suffield to be 13·67 lb./in.^{2} or as 14·7 at sea level. The validity of this scaling procedure is discussed in §6. At 0·1 ft. intervals of scaled distance, within the range covered by the movement of a specific smoke element, the fitted displacement-time equation was solved and differentiated to give a series of distance-time-velocity co-ordinates. The resulting co-ordinates for all the smoke elements were sorted so as to gather the velocity-time pairs for each of the specified distances. A typical set of such data obtained in an experiment with a 200000 lb. surface burst charge is plotted in figure 5 where the given times are measured from the arrival of the shock at that distance.

The error of a least squares fit is normally greatest at the limits of the data and so the derivatives at the extremes of the fitted displacement-time curves were rejected. Values of the particle velocity immediately behind the shock were not obtained therefore. In order to derive this peak value it was necessary to extrapolate the velocity-time co-ordinates to the time of shock arrival and this could be done most consistently and conveniently by fitting an equation to these values. This had the

added advantage that the resulting equation could be used to describe the shape of the velocity decay in a concise form.

The equation which has been used most commonly to describe the decay of blast waves is a modified form of an equation discussed by Friedlander (1946), namely

$$P = P_s(1 - t/\tau)\,e^{-\alpha t},$$

where P is the blast parameter under discussion, P_s its value immediately behind the shock, t the time measured from the shock arrival, α a decay constant, and τ the positive duration at which time the parameter first returns to its ambient value.

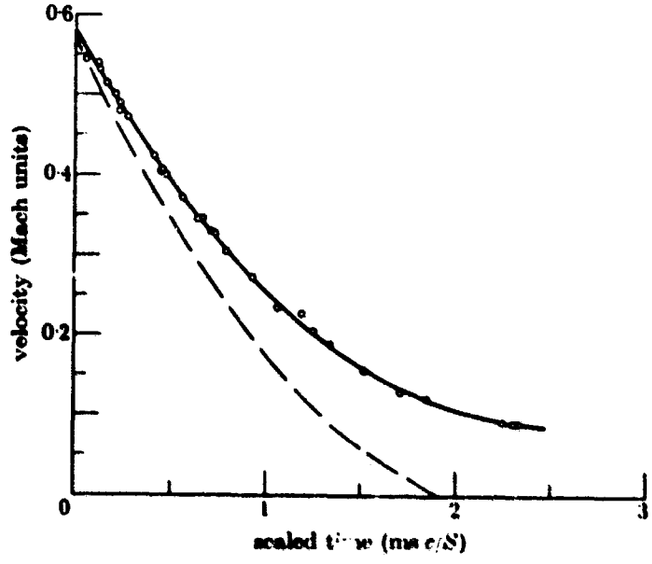

FIGURE 5. Variation of velocity with time at a scaled distance of 7·6 ft./S.
Points (○) are the observed values, solid line is the fit to

$$V = V_s(1 - \beta t)\,e^{-\alpha t} + a \ln(1 + \beta t);$$

broken line is the variation predicted from Brode's calculations.

It can be shown that this equation may be used to describe the decay of some blast parameters from t.n.t. explosions within limited regions, but when attempts were made to fit the velocity data, it became clear that there was a significant departure from the Friedlander form. A good fit could usually be obtained in the region close to the shock and this gave a value of peak velocity which agreed well with the value derived from the shock velocity. Fits could not be obtained at later times. Any reasonable form of the equation significantly underestimated the velocities in this period, and it became clear that an extended form of the equation would be required to describe completely the velocity decay. Some of the equations investigated were

$$V = a + A\,e^{-\alpha t},$$

$$V = V_s[a\,e^{-\alpha t} + (1 - a)\,e^{-\gamma t}](1 - \beta t),$$

and

$$V = V_s(1 - \beta t)\,e^{-\alpha t} + at^n.$$

where a, A, β, γ and n were additional fitted parameters. Consideration of the difference between the observed and the predicted flow, which is discussed below (see §6), indicated an additional logarithmic term, and the equations

$$V = V_s(1-\beta t)\,e^{-\alpha t} + a\ln(1+t),$$

$$V = V_s(1-\beta t)\,e^{-\alpha t} + a\ln(1+\gamma t),$$

and

$$V = V_s(1-\beta t)\,e^{-\alpha t} + a\ln(1+\beta t)$$

were all fitted, each giving a progressively better fit, as judged by the standard error. The excellent way in which this last equation fits the data in figure 5 is typical of that throughout the region studied, and for all charge masses that have been used.

4. Curve-fitting methods

Equations such as those discussed above cannot be fitted to experimental data by usual least squares methods since the normal equations contain the relevant coefficients in non-linear form. An iterative technique was therefore developed, based on a method of Gauss and described, among others, by Whittaker & Robinson (1924), and Moore & Zeigler (1960). Consider a function $y = f(a,b,c,x)$ where x is the independent variable and a, b and c are the parameters for which it is required to obtain a best fit. If $F = \Sigma[\hat{y} - f(a,b,c)]^2$, where $\hat{y}$ is the observed dependent variable, it is required to solve the equations

$$\frac{\partial F}{\partial a} = \frac{\partial F}{\partial b} = \frac{\partial F}{\partial c} = 0.$$

Since these equations could not be solved, estimates a', b', c' of a, b, c were obtained and the function expanded by a Taylor series about this point, namely

$$f(a'+\alpha, b'+\beta, c'+\gamma, x) = f(a', b', c', x) + \left[\alpha\frac{\partial}{\partial a} + \beta\frac{\partial}{\partial b} + \gamma\frac{\partial}{\partial c}\right] f(a', b', c', x)$$

plus higher order terms which may be neglected if α, β and γ are small; that is, if the estimates a', b' and c' are good. The normal equations are then derived as follows:

Let

$$F = \sum_{i=1}^{n} [f(a'+\alpha, b'+\beta, c'+\gamma, x_i) - \hat{y}_i]^2;$$

hence

$$\frac{\partial F}{\partial \alpha} = 2\sum_{i=1}^{n} [f(a'+\alpha, b'+\beta, c'+\gamma, x_i) - \hat{y}_i]\frac{\partial f}{\partial a_i} = 0 \quad \text{for a minimum,}$$

and similarly for $\partial F/\partial b$ and $\partial F/\partial c$.

Applying the approximate value from the Taylor expansion, we have

$$\sum_{i=1}^{n}\left[f(a', b', c', x_i) + \alpha\frac{\partial f}{\partial a_i} + \beta\frac{\partial f}{\partial b_i} + \gamma\frac{\partial f}{\partial c_i} - \hat{y}_i\right]\frac{\partial f}{\partial a_i} = 0, \quad \text{etc.},$$

which gives the normal equations

$$\alpha\Sigma\left(\frac{\partial f}{\partial a_i}\right)^2+\beta\Sigma\left(\frac{\partial f}{\partial a_i}\right)\left(\frac{\partial f}{\partial b_i}\right)+\gamma\Sigma\left(\frac{\partial f}{\partial a_i}\right)\left(\frac{\partial f}{\partial c_i}\right)=\Sigma[y_i-f(a',b',c',x_i)]\frac{\partial f}{\partial a_i},$$

$$\alpha\Sigma\left(\frac{\partial f}{\partial a_i}\right)\left(\frac{\partial f}{\partial b_i}\right)+\beta\Sigma\left(\frac{\partial f}{\partial b_i}\right)^2+\gamma\Sigma\left(\frac{\partial f}{\partial b_i}\right)\left(\frac{\partial f}{\partial c_i}\right)=\Sigma[y_i-f(a',b',c',x_i)]\frac{\partial f}{\partial b_i},$$

$$\alpha\Sigma\left(\frac{\partial f}{\partial a_i}\right)\left(\frac{\partial f}{\partial c_i}\right)+\beta\Sigma\left(\frac{\partial f}{\partial b_i}\right)\left(\frac{\partial f}{\partial c_i}\right)+\gamma\Sigma\left(\frac{\partial f}{\partial c_i}\right)^2=\Sigma[y_i-f(a',b',c',x_i)]\frac{\partial f}{\partial c_i}.$$

These equations are solved to give values of α, β, γ which are added to the estimates of a, b and c to give new estimates, and the process may be iterated until a minimum value of the standard deviation is obtained to a desired degree of accuracy. For this iterative process to converge it is necessary for α, β and γ to be small, that is, good initial estimates of the parameters must be obtained. This iterative technique was used to fit the observed data to the equation

$$V=V_s(1-\beta t)\,e^{-\alpha t}+a\ln(1+\beta t),$$

and thus find the best fit values of V_s, α, β and a.

5. Results

The initial aims of the studies described here were to develop a method for the measurement of the air velocity in blast waves, and subsequently to use this technique to study the air motion in blast waves from a wide variety of charge sizes. It had been intended to make these measurements in the range of intermediate shock strengths from about 7·5 to 0·5 atm overpressure. At high shock strengths, however, the temperature behind the shock was such that the sulphuric acid droplets, which formed the trails, were vaporized. This effect occurred at shock strengths of about 5 atm overpressure for which the temperature behind the shock is 300 °C. Luchinskii (1956) gives the boiling-point of sulphuric acid formed from a water vapour + sulphur trioxide mixture as being in a range from 280 to 339 °C, depending on the percentage of water present. The temperature behind the shock at this pressure level increases with distance from the shock front (Brode 1959), which would account for the observation that, in the limiting region for this effect, the trails do not disappear at the shock, where the overpressure is greatest, but at some distance behind the shock. The majority of air velocity measurements have therefore been restricted to the region of shock strengths from 5 to 0·5 atm overpressure. In current work titanium tetrachloride is being used as a tracer, and satisfactory results have been obtained at higher pressures.

The air velocity was measured in blast waves produced by surface burst charges of t.n.t. of the following masses: 30, 60, 1000, 10000, 40000 and 200000 lb. All the charges were made from cast pure t.n.t. with central Tetrytol boosters. The boosters accounted for about 0·2 % of the charge mass. The 30 and 60 lb. charges were cast as solid spheres, while the large charges were built in the form of hemispheres from

12 in. × 12 in. × 4 in. cast blocks, each of about 32·6 lb. The manufacture of the charges has been described by Pennie, Philips & Holdsworth (1960) and Philips, Ditto & Holdsworth (1960). In all experiments using block-built charges, probes were placed throughout the explosive and uniform detonation was confirmed in all cases.

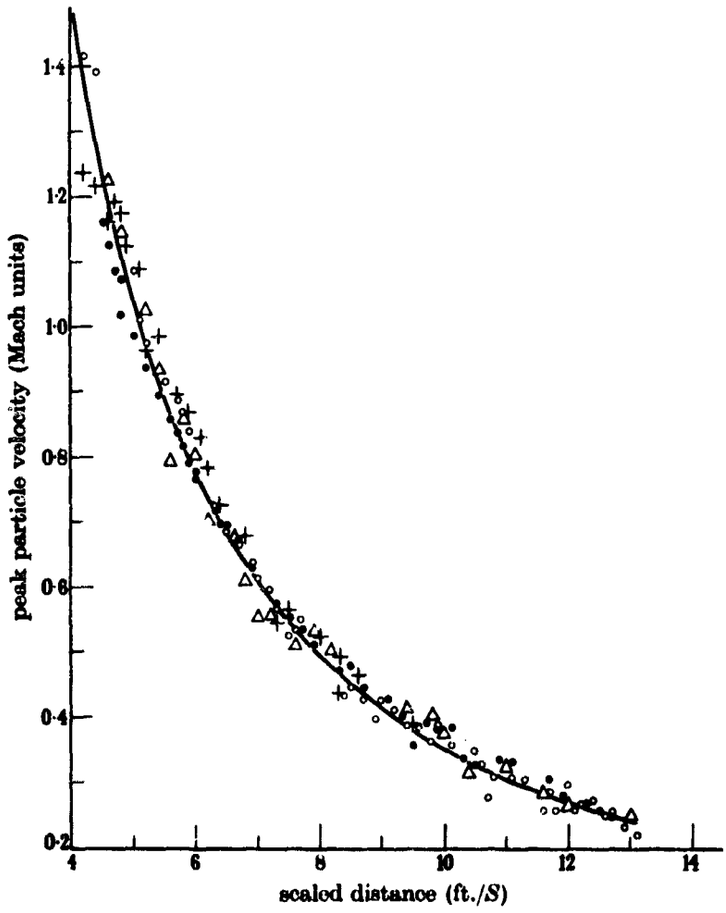

FIGURE 6. Comparisons of peak particle velocities for surface burst t.n.t. charges of 60 lb. (△); 10000 lb. (+); 40000 lb. (○) and 200000 lb. (●). The line shows the particle velocity calculated from the shock velocity.

The results from all experiments were analyzed by the methods described in §§3 and 4, and the values of the peak velocity, V_s, determined by the best fit equation to the velocity-time data are plotted against scaled distance in figure 6. Also shown is the variation of peak particle velocity determined by applying the observed shock velocity in the continuity equations. The variation of velocity with time at specific distances has also been compared with Brode's calculation and a typical comparison was shown in figure 5. Several significant differences may be observed between the two curves. The actual rate of decay of the velocity is slower than that indicated by Brode and the arrival of the secondary shock is sooner, but, due to the extended outward flow from the charge, it occurs in the positive flow

period. There is an indication from some experiments that the flow velocity may increase slightly prior to the arrival of the secondary shock, but this has not been confirmed. The reason for this difference will be discussed (see §6). The secondary shock occurs in the blast wave from a chemical explosion, and originates as an inward facing shock produced by the deceleration of the contact surface between the detonation products and the atmosphere. This shock implodes at the origin and is then reflected outward, to following primary shock, as shown in figure 8.

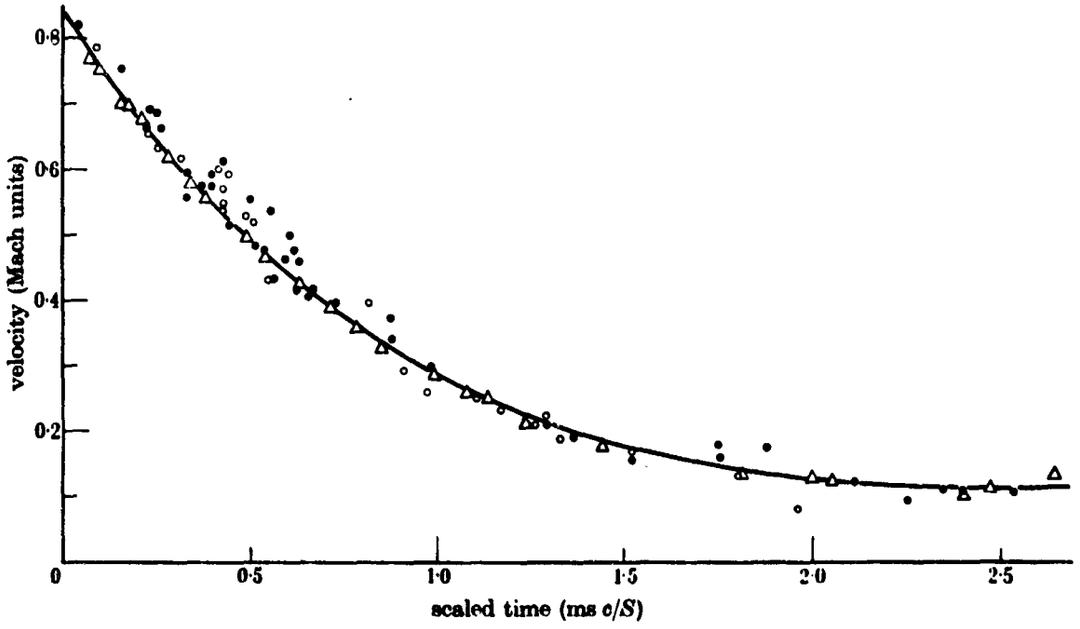

FIGURE 7. Comparison of the time variation of velocity at a scaled distance of 5·8 ft./S from surface burst t.n.t. charges of 60 lb. (○); 40000 lb. (●) and 200 000 lb. (△). The line is the least squares fit to the 200000 lb. data.

Comparisons were also made between the velocity-time variations obtained using the different explosive yields, and typical comparisons at a specific scaled distance are shown in figure 7. At no distances could any significant differences be observed and the data for all the experiments could therefore be combined and fitted to

$$V = V_a(1-\beta t)e^{-\alpha t} + a\ln(1+\beta t).$$

The resulting best fit values of V_a, α, β, a and t^* are given in table 1, where t^* is the time for the velocity to fall to V_a/e. This latter parameter is given since it has more physical significance than $1/\beta$ which should not be considered as the positive duration in this case but rather as a normalizing factor for time.

All of the information derived by the smoke trail experiments may be presented on a single $x-t$ diagram, as shown in figure 8. This information includes the distance versus time of the primary and secondary shocks, particle trajectories as traced by individual smoke elements, the isotachs joining points of equal velocity and the distance variation of t^*.

TABLE 1. BEST FIT PARAMETERS OF EQUATION $V = V_e e^{-\alpha t}(1-\beta t) + a \ln(1+\beta t)$

scaled distance (ft./lb.$^{\frac{1}{3}}$)	peak velocity, V_e (Mach units)	α	β	a	t^*
5·0	1·02	0·520	1·242	0·545	0·83
5·5	0·88	0·460	1·174	0·500	0·89
6·0	0·78	0·415	1·162	0·467	0·97
6·5	0·69	0·374	1·140	0·437	1·05
7·0	0·61	0·343	1·131	0·410	1·12
7·5	0·55	0·318	1·118	0·384	1·18
8·0	0·50	0·300	1·101	0·360	1·23
8·5	0·46	0·290	1·070	0·332	1·27
9·0	0·42	0·279	1·065	0·313	1·32
9·5	0·39	0·268	1·043	0·294	1·39
10·0	0·36	0·258	1·030	0·276	1·44
10·5	0·33	0·246	1·020	0·264	1·51
11·0	0·31	0·238	1·007	0·252	1·56
11·5	0·29	0·228	0·998	0·239	1·60
12·0	0·27	0·220	0·989	0·229	1·63
12·5	0·26	0·211	0·980	0·220	1·66
13·0	0·24	0·206	0·975	0·210	1·68

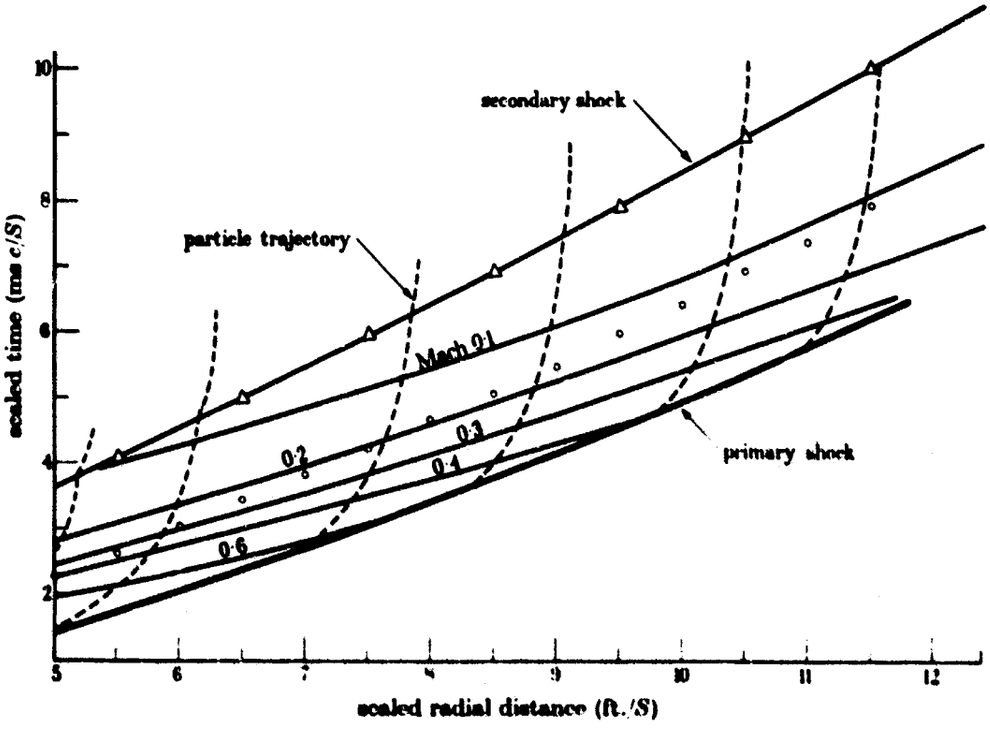

FIGURE 8. x–t diagram showing the trajectories of the primary (——) and secondary (-Δ-) shocks; the particle trajectories (· · · ·); the isotachs (– – –) joining points of equal Mach velocity and t^*(○), the time at which the velocity has decayed to $1/e$ of its peak value.

6. Discussion

The technique for the measurement of air velocity in blast waves has been developed to a stage at which it can be applied to free-field measurements on a routine basis, and with inherent errors not larger than those of other blast measurements. The smoke is observed inside the shock sphere so that light from the trails is refracted continuously in its passage through the high-density region behind the shock, and also, in the opposite direction, at the front itself. This refraction will give a slight shift to the image of the trail, but calculations based on an assumed density variation behind the shock indicated that the apparent displacement would be less than 0·1 % in the region of interest and, in fact, only 0·3 % at a shock strength of 200 atm. This point was also checked experimentally by attempting to detect any apparent shift of the marker boards as they were enveloped by the wave. No such a shift could be measured.

The peak velocities and the variation of velocity with time at specific distances from the charge have been compared with the predictions for a t.n.t. explosion, given by Brode (1959), who based his calculations on an energy release of 1 kcal. He assumed a figure of 252 kcal/mole for t.n.t. with a density of 1·5 g/cm^3, which gives a scaling factor of 9·4 for a 1 lb. charge. A random selection of 813 cast t.n.t. blocks from those used to build the charges for the experiments described above, had a mean density of 1·57 g/cm^3. For cast t.n.t. of this density, Cook (1958) quotes an energy yield of 1·16 kcal/g which gives a scaling factor of 9·6 applicable to Brode's results for a 1 lb. charge. Measurements of peak pressure have been made by Groves (personal communication) for a large number of air-burst spherical t.n.t. charges, using a photogrammetrical method of determining the shock velocity. The pressure distance curve from these experiments is shown in figure 9. A comparison with corresponding results by Brode gives a scaling factor of 10·0, and this factor has therefore been used for all the air velocity comparisons. It would appear that the energy yield of t.n.t. detonated in free air may be about 4 % greater than that indicated by Cook.

The air velocity measurements described here were made with surface burst charges, and to compare these results with predictions for a free air spherical explosion, it was necessary to apply a ground reflexion factor. This was done by comparing the shock overpressure-distance relationships of air and ground burst charges and finding the ratio of the distances at which a specific pressure was observed. The cube of this ratio gives a reflexion factor which, for a perfectly reflecting surface would be two. Figure 9 shows such a comparison which yields reflexion factors that vary in the region of present interest from 1·5 to 1·76, depending on the distance from the charge. The comparisons between the observed and predicted velocities have been made using the appropriate reflexion factor calculated in this way. To confirm the validity of this procedure the air velocity was measured in the blast waves from spherical t.n.t. 60 lb. charges detonated at 45 ft. above the ground. Comparisons between the free air and surface bursts results scaled in this way, are shown in figure 10 and no significant difference can be observed.

When it became clear that the decay of air velocity in blast waves from t.n.t.

explosions was not following the expected form, comparisons were made between the observed velocity decay and that derived from Brode's calculations.† Such a comparison was shown in figure 5. The difference between the observed and predicted velocities was studied and found to yield a consistent relationship of the form $\Delta v = a \ln(1+\beta t)$ where Δv is the velocity difference (see figure 11). Combination with the modified Friedlander equation led directly to the form quoted above. It must be pointed out that this equation is empirical and no physical significance can be attached to any of the fitted parameters, other than V_s, the peak velocity.

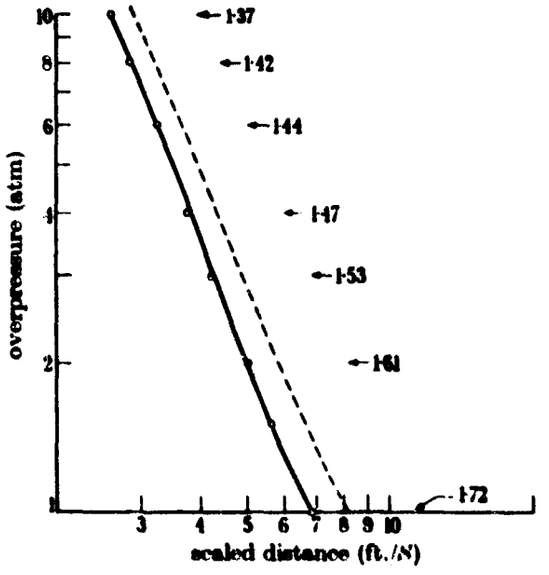

FIGURE 9. Variation of peak overpressure with distance from the charge. Solid line is the free air relationship. The broken line is a relationship for a surface burst charge. The numbers against the arrows are reflexion factors at the specified pressures. The points (O) are derived from Brode's calculations for a scaling factor of 10·0.

It is suggested that the departure of the velocity decay from that of a classical blast wave is due to 'after-burning' of t.n.t. Trinitrotoluene has a chemical composition of the form $C_7H_5N_3O_6$. Cook (1958) gives the detonation products of 1·59 density t.n.t. as carbon monoxide (1), carbon dioxide (10), water (1), nitrogen (5·9), ammonia (0·4), methyl alcohol (4·5), hydrogen cyanide (1·1) and carbon (14·2) where the figures in brackets are the number of moles per kilogramme. Although the exact composition of these products will depend on the nature of confinement of the explosive (Jones & Miller 1948), a simplified analysis, assuming stoichiometric mixtures indicates an oxygen deficiency of greater than 60 % by mass. On several of the large-scale experiments radiation measurements were made to determine fireball black-body temperatures, such as those described by Tate & Pattman (1962)

† The report of Brode's calculations for t.n.t. quotes the variation of blast parameters with distance from the explosion, at specific times. For practical studies of blast waves it is usually more convenient to know the variation with time at specific locations. Dr Brode was kind enough to lend his original computer outputs to the author, so that the required information could be derived and used in the comparisons discussed here.

for a 100 ton t.n.t. explosion. These measurements showed a peak temperature of 8600 °K at 0·7 ms after detonation, which may be associated with the shock front temperature. As the shock front expanded and cooled it became transparent to the

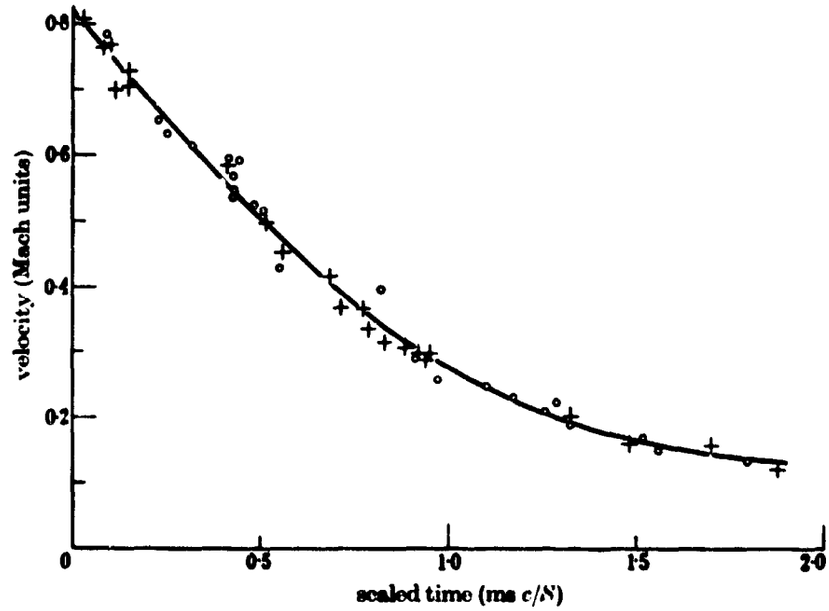

FIGURE 10. Comparison of the velocity-time variations from free air and surface burst 60 lb. t.n.t. charges. +, Free air measurement at a scaled distance of 4·8 ft./S; ○, surface burst measurement at a scaled distance of 5·8 ft./S; line shows the least squares fit to the combined data.

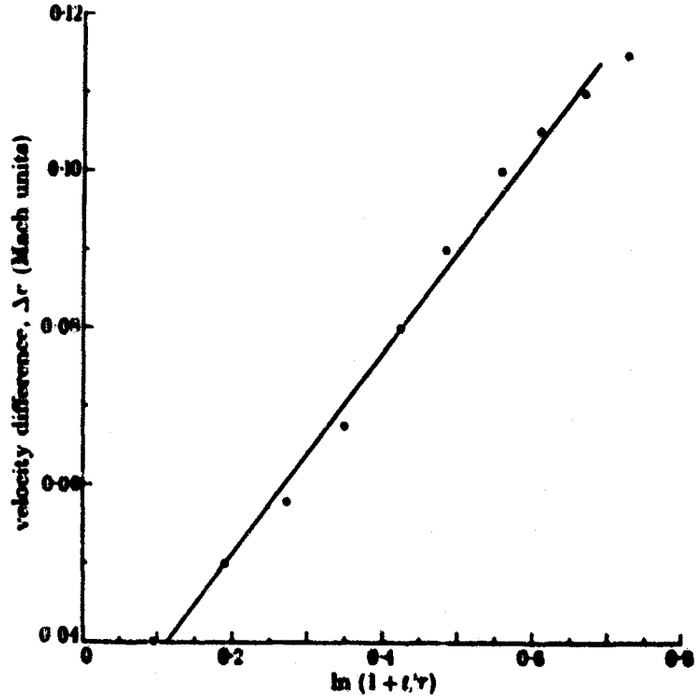

FIGURE 11. Difference between the predicted (Brode) and observed particle velocities plotted against ln $(1+t/\tau)$. τ is the duration of the predicted positive flow.

radiation from the detonation products, yielding a black-body temperature of about 3000 °K. These products continued to radiate for several seconds after detonation at a temperature of about 2500 °K. It therefore appears that the detonation products are of a composition and temperature such that several exothermic reactions will take place in the presence of atmospheric oxygen, thus serving as a relatively slow but significant energy source for some time after detonation. It is suggested that this additional release of energy accounts for the non-classical decay of velocity within the blast wave.

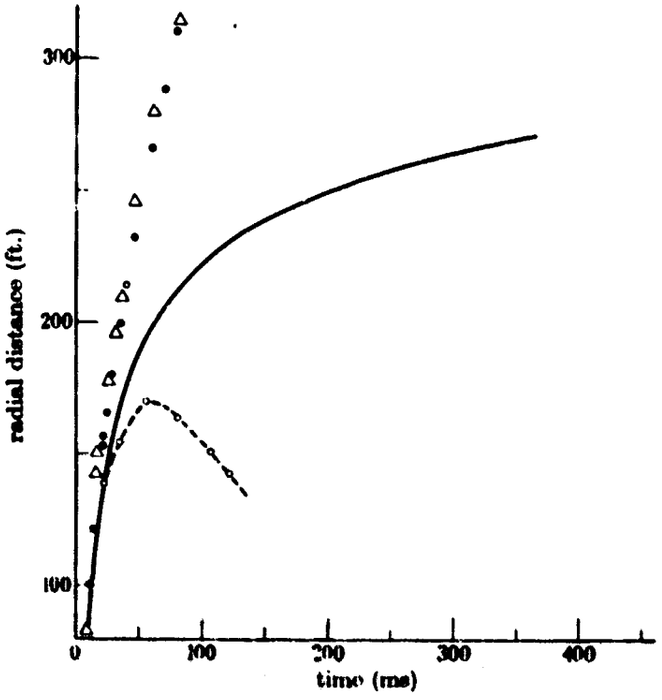

FIGURE 12. Comparison of the observed and predicted contact surface trajectories for a 200000 lb. t.n.t. surface burst charge. Solid line shows the observed trajectory and the broken line the trajectory predicted from Brode's calculations. Points are the observed (●) and predicted (△) main shock trajectories.

This effect is further illustrated by a comparison between the observed growth of the fireball and the trajectory of the contact surface predicted by Brode. Such a comparison is shown in figure 12. It will be seen that there is excellent agreement between the two shock trajectories, indicating that the correct scaling factor has been used, but a considerable difference between the trajectories of the two contact surfaces indicates a process such as 'after-burning' for which no allowance was made in Brode's calculations. This phenomenon also has been observed when explosives of low oxygen balance are used for shallow blasting. When the combustion products escape and mix with the atmosphere, a secondary explosion occurs.

In order to test this 'after-burning' hypothesis, it would be desirable to study the blast waves produced by t.n.t. charges detonated in an oxygen-free atmosphere. However, pure t.n.t. cannot be detonated easily in masses less than about 8 lb.,

and facilities for performing such an experiment are not at present available. An alternative was to make measurements in blast waves produced by explosives with a high oxygen balance, such as nitroglycerine. Cook (1958) gives the detonation products of nitroglycerine, with a specific gravity of 1·6, as carbon dioxide (13·2), water (11), nitrogen (5·9), nitric oxide (1·4) and oxygen (0·4) where the figures in brackets indicate moles per kilogramme. The high sensitivity of this explosive makes it difficult to use for experimental purposes, but a series of experiments was carried out with 60 lb. spherical charges of Geogel, an explosive produced by Canadian

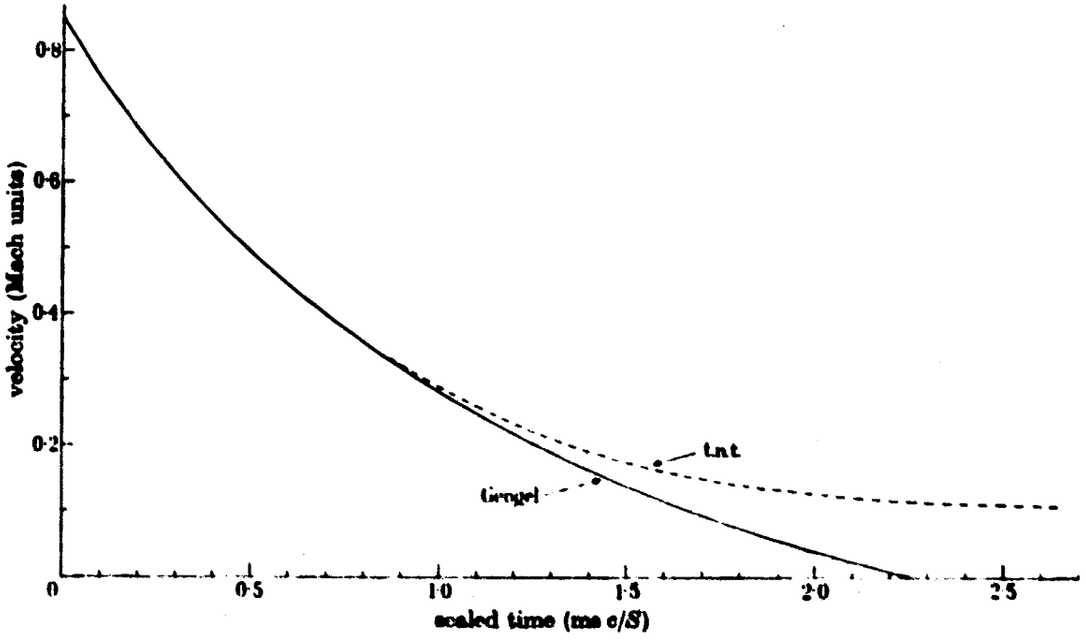

FIGURE 13. Comparison of the velocity-time variations at a scaled distance of 5·8 ft./S from 60 lb. surface burst charges of t.n.t. and Geogel.

Industries Ltd. and composed of 50 % nitroglycerine. The manufacturers quoted an energy yield 1 % higher than t.n.t. and a 2·5 % excess of oxygen in the explosive products. The pressure-distance curves obtained for air burst and ground burst Geogel charges had a different slope from those of t.n.t. with a cross-over point at about 1·75 atm, corresponding to a distance of about 6 ft. from a 1 lb. charge. Closer to the charge the pressures from t.n.t. were greater and at longer distances they were less than those for Geogel. This was to have been expected from the slower detonation velocity of Geogel quoted at 6300 m/s compared with 6650 m/s for t.n.t. For convenience, comparisons between the air velocities in the two blast waves were made close to this cross-over point. Figure 13 shows a comparison between the velocity-time variations for t.n.t. and Geogel. There is no measurable difference between the two decays until the velocity has fallen to about Mach 0·2, from which point the Geogel curve continues to fall in the classical manner, giving a scaled positive duration of about 2·3. The difference between the blast waves from the two explosives is shown even more clearly by the comparison between the particle trajectories shown in figure 14.

In a series of experiments with 60 lb. t.n.t. and Geogel charges, the detonations were photographed at 64 frames/s on a colour film. A luminous fireball from the t.n.t. explosions existed for at least 500 ms, but for less than 17 ms for the Geogel.

It was recently brought to the author's attention that a limited number of smoke puffs and trails had been used on some of the early nuclear explosions detonated by the United States, and, on request, a copy of a 100 frames/s film showing the smoke movement, was supplied by the U.S. Government. The small number of smoke trails that had been used did not make possible a complete particle velocity analysis,

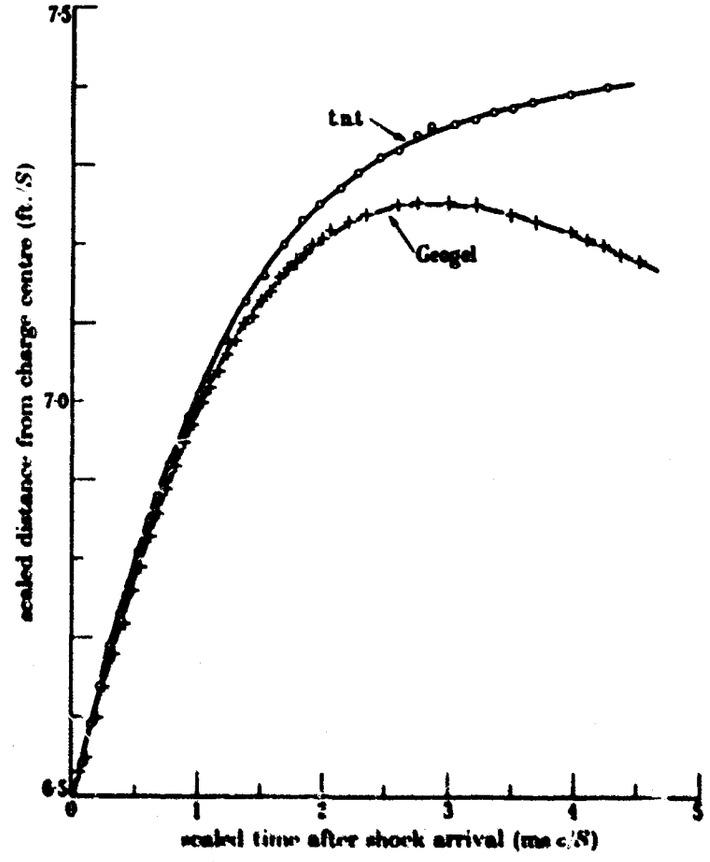

FIGURE 14. Comparisons of the particle trajectories in blast waves from 60 lb. surface burst charges of t.n.t. (○) and Geogel (+).

but several particle trajectories could be followed. Analysis of the shock velocity from the nuclear explosion indicated a blast yield of about 32 kilotons. This figure was used to scale the results so that they could be compared with t.n.t. data, and such a comparison is shown in figure 15. The initial scaled particle displacements from the two explosions are very similar, but differ significantly at later times when the nuclear blast decays in the classical form. Both curves were derived from free air explosions and discontinuities are caused by the arrival of the shock reflected from the ground.

Taylor (1950) pointed out that a major difficulty in the analysis of spherical blasts is that the shock wave leaves the air in a state in which the entropy decreases

radially, so that after its passage, when the air has returned to atmospheric pressure, the air temperature decreases with increasing distance from the centre of the explosion. For this reason the density is not a single valued function of the pressure in a blast wave, and if the pressure-time relation is measured at a point, it is not possible to derive directly the density-time relation unless the particle trajectories are known. In this case the trajectory of the air which was monitored by the pressure transducer at any instant can be traced back to its position when it was shocked. The Rankine–Hugoniot equation can then be applied at that point and the density at the original position and time calculated from the adiabatic equation.

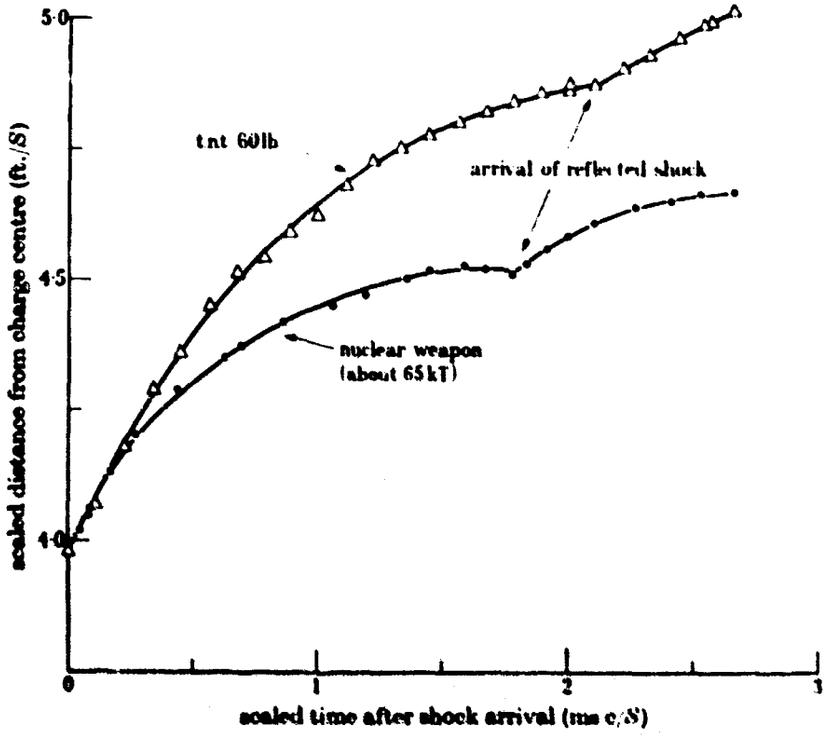

FIGURE 15. Comparisons of the particle trajectories in blast waves from air burst t.n.t. (△) and nuclear (●) explosions.

Such a conversion has, in fact, been done with reasonable success (Dewey & Anson 1963). On the other hand, if the particle trajectories are known, it is possible to calculate the density directly in terms of the ambient value by applying the conservation of a mass equation which is unaffected by the entropy change at the shock. The equation may be written for a spherical flow in the form

$$\frac{\rho}{\rho_0} = \frac{x^2}{r^2}\frac{1}{(\partial r/\partial x)},$$

where ρ_0 is the ambient density and ρ the density of an air element at a time t and radial position r, the original position of which was x. The partial derivation $\partial r/\partial x$ may be determined from the observed relationship between r and x at a constant time. A family of such curves for a 200 000 lb. t.n.t. explosion is shown in figure 16.

The hydrostatic pressure may now be determined from the density by using the adiabatic equation as described above. The velocity of sound and thus temperature ratios can then be found. This would be of great advantage since it would enable velocity methods to be applied to reflected and secondary shocks. The application of the above relations requires the assumption of a constant ratio of specific heats throughout the wave, and this is probably valid for blast waves of strengths less than about seven atmospheres overpressure. These relations have been applied in

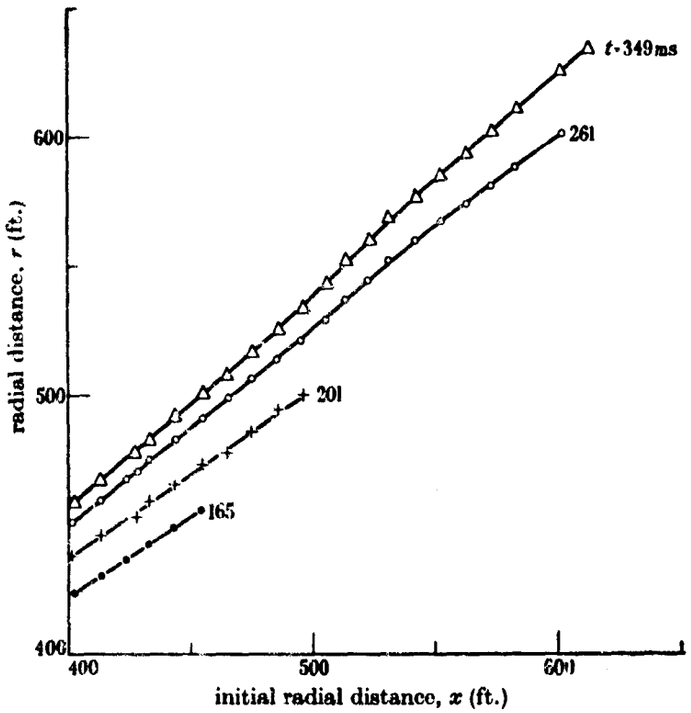

FIGURE 16. The radial positions (r) of elements in a blast wave plotted against their original positions (x) at the stated times (t). Data obtained with a 200 000 lb. surface burst charge. The slopes of these curves are a measure of the radial compression from which the density ratio can be calculated.

preliminary hand calculations which showed good agreement with the pressures and densities measured independently. Such an analysis is well suited to a digital computer and would permit a complete description of all the physical parameters within a blast wave in the range discussed, using only photographic instrumentation.

7. CONCLUSIONS

The smoke trail displacement technique has enabled the particle velocities to be measured in blast waves from t.n.t. explosions varying in mass from 30 to 200 000 lb. Throughout this range the results have scaled completely, using a factor

$$S = \sqrt[3]{(WP_0/P)},$$

where W is the charge mass, P the ambient pressure and P_0 a standard pressure. Good scaling was also achieved between air burst and ground burst explosions by

using a ground reflexion factor in the range of 1·5 to 1·76, depending on the distance from the charge. There was no significant difference between the measured velocities close to the shock and those predicted from Brode's (1959) calculations after applying a scaling factor of 10·0 for a 1 lb. charge. At later times the decay of velocity did not follow the classical form and there was an extended outward flow from the charge. The shape of the velocity decay could be described by an empirical equation of the form

$$V = V_s e^{-\alpha t}(1-\beta t) + a \ln(1+\beta t).$$

It is postulated that the extended flow is due to the after-burning of the t.n.t. detonation products in the presence of atmospheric oxygen, and it has been shown that this phenomenon does not occur for an explosive with a high oxygen balance or for a nuclear explosion. It has been shown that for the range of shock strengths studied, it is possible, in theory, to determine the time and spatial variation of all the physical parameters of blast waves from the photographic analysis of the particle trajectories. These analyses will be the object of future studies.

The work described here was carried out as part of a programme of the Defence Research Board of Canada whose permission to publish this paper is gratefully acknowledged. Research of this nature requires the assistance of a very large number of persons and, the author wishes to thank, in particular, the Suffield Field Section under the leadership of Mr N. Spackman, the Munitions Section under Mr W. Ditto for provision of the explosive charges, black smoke background and the smoke mortars, Photography Section under Mr F. C. Trafford for provision of the excellent photographic records and, above all, Mr W. A. Anson for his unfailing assistance at all stages of this work.

References

Brode, H. L. 1955 *J. Appl. Phys.* **26**, no. 6.
Brode, H. L. 1956 *Rand Corp. Rep.* RM–1825–AEC.
Brode, H. L. 1959 *Phys. Fluids*, **2**, no. 2.
Broyles, C. D. 1960 *Sandia Corp. Tech. Rep.* 268–56–51.
Cook, M. A. 1958 *The science of high explosives.* New York: Reinhold Publ. Corp.
Dewey, J. M. & Anson, W. A. 1963 *J. Sci. Instr.* **40**, 568–572.
Friedlander, F. G. 1946 *Proc. Roy. Soc.* A, **186**, 322.
Jones, H. & Miller, A. R. 1948 *Proc. Roy. Soc.* A, **194**, 480.
Luchinskil, G. P. 1956 *Zhur. Fiz. Khim.* **30**, 1207–22.
Moore, R. H. & Zeigler, R. K. 1960 *Los. Alamos Rep.* LA-2367.
Muirhead, J. C. & Lecuyer, D. W. 1959 *Suffield Tech. Note*, no. 36.
Muirhead, J. C., Lecuyer, D. W. & McCallum, F. L. 1959 *Suffield Tech. Pap.*, no. 153.
Muirhead, J. C. & McCallum, F. L. 1959 *Suffield Tech. Pap.*, no. 159.
Oshima, K. 1960 *Aero. Res. Inst., Univ. Tokyo, Rep.*, no. 358.
Pennie, A. M., Phillips, A. C. & Holdsworth, J. 1960 *Suffield Tech. Pap.*, no. 190.
Philips, A. C., Ditto, W. J. & Holdsworth, J. 1960 *Suffield Tech. Pap.*, no. 194.
Sakurai, A. 1953 *J. Phys. Soc. Japan*, **8**, no. 5.
Sakurai, A. 1954 *J. Phys. Soc. Japan*, **9**, no. 2.
Ström, L. 1962 *Trans. Chalmers Univ. Tech* (*Sweden*), no. 259.
Tate, P. A. & Pattman, J. D. R. 1962 *Def. Res. Chem. Lab.* (*Ottawa*) *Rep.* no. 371.
Taylor, Sir Geoffrey 1950 *Proc. Roy. Soc.* A, **201**, 159–186.
Von Neumann, J. & Bethe, H. A. 1958 *Los Alamos Rep.* no. LA-2000.
Whittaker, E. & Robinson, G. 1924 *The calculus of observations.* London: Blackie and Sons.